

University of New Hampshire

University of New Hampshire Scholars' Repository

New Hampshire Agricultural Experiment Station Publications New Hampshire Agricultural Experiment Station

6-28-2017

Bacterial community profiles and *Vibrio parahaemolyticus* abundance in individual oysters and their association with estuarine ecology

Ashley L. Marcinkiewicz
University of New Hampshire, Durham

Brian M. Schuster
University of New Hampshire, Durham

Stephen H. Jones
University of New Hampshire, Durham, Stephen.Jones@unh.edu

Vaughn S. Cooper
University of Pittsburgh

Cheryl A. Whistler
University of New Hampshire, Durham, cheryl.whistler@unh.edu

Follow this and additional works at: <https://scholars.unh.edu/nhaes>

Comments

This article is a preprint and has not been peer-reviewed.

Recommended Citation

Marcinkiewicz, Ashley L.; Schuster, Brian M.; Jones, Stephen H.; Cooper, Vaughn S.; and Whistler, Cheryl A., "Bacterial community profiles and *Vibrio parahaemolyticus* abundance in individual oysters and their association with estuarine ecology" (2017). *New Hampshire Agricultural Experiment Station Publications*. 333.

<https://scholars.unh.edu/nhaes/333>

This Article is brought to you for free and open access by the New Hampshire Agricultural Experiment Station at University of New Hampshire Scholars' Repository. It has been accepted for inclusion in New Hampshire Agricultural Experiment Station Publications by an authorized administrator of University of New Hampshire Scholars' Repository. For more information, please contact Scholarly.Communication@unh.edu.

1 Bacterial community profiles and *Vibrio parahaemolyticus* abundance in individual oysters and
2 their association with estuarine ecology

3

4 Ashley L. Marcinkiewicz^{1,2,3}, Brian M. Schuster^{2,4}, Stephen H. Jones^{1,5}, Vaughn S. Cooper^{1,2,6}
5 and Cheryl A. Whistler^{1,2*}

6 ¹ Northeast Center for Vibrio Disease and Ecology, University of New Hampshire, Durham, NH,
7 USA

8 ² Department of Molecular, Cellular, and Biomedical Sciences, University of New Hampshire,
9 Durham, NH, USA

10 ³ Current Address: New York State Department of Health, Wadsworth Center, Albany, NY,
11 USA

12 ⁴ Current Address: Seres Therapeutics, Cambridge, MA, USA

13 ⁵ Department of Natural Resources and the Environment, University of New Hampshire,
14 Durham, NH, USA

15 ⁶ Current Address: Department of Microbiology and Molecular Genetics, University of
16 Pittsburgh School of Medicine, Pittsburgh, PA, USA

17 * Corresponding author: cheryl.whistler@unh.edu

18

19

20

21

22

23

24 **ABSTRACT**

25 Oysters naturally harbor the human gastric pathogen *Vibrio parahaemolyticus*, but the nature of
26 this association is unknown. Because microbial interactions could influence the accumulation of
27 *V. parahaemolyticus* in oysters, we investigated the composition of the microbiome in water and
28 oysters at two ecologically unique sites in the Great Bay Estuary, New Hampshire using 16s
29 rRNA profiling. We then evaluated correlations between bacteria inhabiting the oyster with *V.*
30 *parahaemolyticus* abundance quantified using a most probable number (MPN) analysis. Even
31 though oysters filter-feed, their microbiomes were not a direct snapshot of the bacterial
32 community in overlaying water, suggesting they selectively accumulate some bacterial phyla.
33 The microbiome of individual oysters harvested more centrally in the bay were relatively more
34 similar to each other and had fewer unique phylotypes, but overall more taxonomic and
35 metabolic diversity, than the microbiomes from tributary-harvested oysters that were
36 individually more variable with lower taxonomic and metabolic diversity. Oysters harvested
37 from the same location varied in *V. parahaemolyticus* abundance, with the highest abundance
38 oysters collected from one location. This study, which to our knowledge is the first of its kind to
39 evaluate associations of *V. parahaemolyticus* abundance with members of individual oyster
40 microbiomes, implies that sufficient sampling and depth of sequencing may reveal microbiome
41 members that could impact *V. parahaemolyticus* abundance.

42

43 **KEYWORDS:** *Vibrio parahaemolyticus*; oysters; microbiome; 16s rRNA

44 1. Introduction

45 Shellfish, including the eastern oyster (*Crassostrea virginica*), are common vectors for
46 human pathogens. This includes the bacterium *Vibrio parahaemolyticus*, the leading causative
47 agent of bacterial seafood-borne gastroenteritis worldwide and an emergent pathogen in the

48 United States (US) (1). Oysters concentrate *V. parahaemolyticus* from overlaying water, which
49 can lead to a naturally higher abundance than the < 10,000 Most Probable Number (MPN)/g that
50 is currently recommend in the US as a limit to ensure shellfish is safe for consumption (2, 3). To
51 increase shellfish safety, fisheries employ strategies intended to reduce pathogen levels in live
52 product, including depuration in UV sterilized water or relay/transplantation of oysters to a
53 location where *V. parahaemolyticus* is of low abundance, often correlating with high salinity (4,
54 5, 6). But reported correlations of salinity with *V. parahaemolyticus* abundance from
55 environmental studies are mixed (3) suggesting factors other than salinity likely mediate a
56 reduction in *V. parahaemolyticus* concentrations. Furthermore, relay of oysters into non-
57 sterilized water more effectively reduces *V. parahaemolyticus* contamination than depuration in
58 sterile water (6). Therefore, antagonistic relationships among community members coupled with
59 less than favorable salinity conditions could explain the greater reduction of *V. parahaemolyticus*
60 in the oyster microbiome during relay (7, 8).

61 Ecological studies reveal a few biotic factors correlate with *V. parahaemolyticus*
62 abundance both in water and in oysters (3). Zooplankton can positively correlate with *V.*
63 *parahaemolyticus* abundance when they serve either as a nutrient resource or a mechanism of
64 dispersal (3, 9). *V. parahaemolyticus* abundance also positively correlates with chlorophyll *a*,
65 suggesting a general interaction with phytoplankton (3, 8). Oysters could passively accumulate
66 planktonic and particle-associated Vibrios by filter-feeding (3). Even so, the overall oyster
67 microbiome is more diverse than the overlying water microbiome, suggesting potential selective
68 accumulation and culturing of some microorganisms, including Vibrios, by the oyster (10-14). *in*
69 *vitro* bacterial-*Vibrio* competitions illustrate several types of marine bacteria influence *Vibrio*
70 abundance, suggesting *in situ* interactions could influence accumulation in oysters (15-17).

71 Although a growing number of studies have profiled the oyster and overlying water microbiome
72 (18-23), none have yet attempted to correlate presence or abundance of species or community
73 composition profiles to the relative abundance of *V. parahaemolyticus*.

74 To identify the core and variable microbiome among individual oysters, and correlate
75 differences in *Vibrio parahaemolyticus* abundance with microbiome composition, we profiled
76 the microbiome of individual oysters and overlying water from two naturally occurring,
77 ecologically-distinct oyster beds. We employed 454 pyrosequencing of 16s RNA variable region
78 (V2-V3) amplicons, and in parallel quantified *V. parahaemolyticus* abundance. We determined
79 that oysters harbor a microbiome that is distinct from overlying water, and species composition
80 and relative abundance is influenced by location of the oyster bed, potentially reflective of
81 unique ecology. The abundance of *V. parahaemolyticus* varied between oysters and correlated
82 with only a few rare phyla, which were linked to location. The study suggested increased
83 sampling and microbial community sequencing depth could reveal meaningful patterns of
84 association both with ecology and potentially *V. parahaemolyticus* abundance.

85

86 2. Results and Discussion

87 2.1 Sequencing the oyster microbiome

88 To assess the composition of and variation in oyster associated microbiota, native oysters
89 were collected from two ecologically distinct sites, less than five miles apart in the Great Bay
90 Estuary (GBE) of New Hampshire. The Oyster River (OR) oyster bed is located within one of
91 the seven tributaries of this estuary where harvesting is prohibited due to its proximity to the
92 outflow of a municipal wastewater treatment facility (WWTF), whereas the Nannie Island (NI)
93 oyster bed is centrally located within the estuary and is classified as approved for recreational

94 harvesting (8). Thus, these two sites may reveal how the different associated ecological and
95 sewage discharge-related factors pertaining to each site influence the microbial community
96 composition. We generated and sequenced 16s rRNA gene amplicons from total bacterial DNA
97 isolated from ten individual oyster homogenates and one overlying water sample from each
98 collection site. From the generated ~1.5 million reads, only ~1/3 (512,220) with 100% identity to
99 the forward primer and mid-tag were included in the analysis. Quality filtering with FlowClus
100 removed an additional 6,995 reads, producing an average of 18,087 reads per NI oyster (10,338-
101 31,788; n=10), and 29,391 reads per OR oysters (ranging from 9,670-47,231; n=10) for analysis.
102 A lower number of reads were obtained from water – 6495 and 397 from NI and OR,
103 respectively (Supplemental Table 1). Because we seek to determine correlations of identifiable
104 phylotypes with estuarine conditions and *V. parahaemolyticus* abundance, we evaluated in
105 parallel two common pipelines, QIIME and mothur, that use different clustering algorithms, and
106 determined mothur maximized assignment of OTUs at the species level of classification and also
107 resulted in no unclassified reads (Table 1). Therefore, analysis continued with the mothur-
108 generated classified dataset.

109 The rarified phylogenetic distance (PD) whole tree alpha diversity index was applied to
110 illustrate within-sample diversity and evaluate sufficiency in depth of sequencing. Overall higher
111 index values in NI samples indicated higher alpha diversity than OR samples (Fig. 1). However,
112 he plotted rarefactions demonstrated that total phylogenetic distances between all OTUs at each
113 subsampling step continued to increase with higher sampling, indicating that all interpretations
114 should consider that the data did not capture total diversity (Fig. 1).

115

116 2.2 Comparison of the distribution of phylotypes by site and substrate

117 Comparisons of the distribution of OTUs in individual oysters and overlying water can
118 reveal the extent to which the microbiome of individual oysters reflects the microbes in
119 overlying water. Since relatively fewer reads were available from the water samples, it is
120 unsurprising that oysters from both sites harbor OTUs absent in the respective overlying water,
121 (Fig. 2A). Even so, some OTUs from the water samples (1.35% and 0.19% from NI and OR,
122 respectively) were not detected in any oyster, suggesting the potential for some selectivity in the
123 microbiome accumulated from water, which is in agreement with other oyster microbiome
124 studies (18, 25).

125 Comparisons of individual oysters to each other also provided insight into the shared and
126 variable microbiome. Less than 1% of the OTUs identified in any oyster were present in every
127 one of the 20 oysters. However, the shared microbiome from oysters harvested from the same
128 location was slightly larger, with 2.29% OTUs shared between every oyster from NI, and 1.25%
129 shared from OR (Fig. 2B). In addition, 82% of the OTUs shared between every NI oyster were
130 also present in overlying water (1.63% of total OTUs present in any NI oyster), indicating these
131 consistently detected microbiome members at this site are substantially present in and likely
132 influenced by the water column. Because the OR water sample yielded so few sequences for
133 analysis, meaningful comparisons in this case were deemed not possible.

134 Next, we evaluated whether there were informative patterns in the abundance and
135 distribution of phyla-level classifications by dual hierarchical cluster analysis, representing broad
136 scale differences between the microbiome of both sampling sites. Most of the variation between
137 sample type, sites, and even individual oysters was explained by not the high abundance, but the
138 mid- and low abundance phyla (Fig. 3A), and rarifying the sequences to remove the lowest-
139 abundant OTUs, which is a common practice to remove erroneous OTUs (e.g., 20), would have

140 removed most of this potentially informative variation. Phylum-level analysis clearly
141 demonstrated differences between the overlying water and oysters. This analysis also revealed
142 delineation between the microbial communities of oysters by site, when considering both
143 standardized and unstandardized clustering, with only a few exceptions (Fig. 3A-B).

144 The most abundant phyla were consistent with other oyster microbiome studies, even
145 though these were from relatively warmer climates. The major *Crassostrea* sp.-associated phyla
146 include Cyanobacteria, Chloroflexi, Firmicutes, Proteobacteria, Planctomyces, and Bacterioidetes
147 (18, 20, 21). The digestive gland of Sydney rock oysters contains many of these same phyla, and
148 also is dominated by Spirochaetes (23). Cyanobacteria were in higher abundance at NI (33.8%,
149 ranging from 1 to 69%) than OR (7.7%, ranging from 0.8 to 43.0%; Fig. 3B). Whereas some
150 oyster microbiome studies have discarded Cyanobacteria reads to eliminate sequenced
151 chloroplasts from algal matter (20, 21), oysters will ingest Cyanobacteria as a food source (26)
152 and accumulate Cyanobacteria in greater numbers than the surrounding water column (18),
153 justifying retention of these reads as part of the microbiome. Cyanobacteria may even influence
154 the abundance of other members of the oyster microbiome. For instance, Proteobacteria,
155 Bacterioidetes, and Firmicutes have all been isolated from cyanobacterial blooms (27). Therefore,
156 it is possible that differences in microbial community composition between NI and OR were
157 influenced, at least in part, by the overall higher abundance of Cyanobacteria at NI.

158 Whereas differential abundances in broad phyla-level classifications reveal general
159 patterns, considering all taxonomic levels with Unifrac uncovered more specific relationships
160 between samples (Fig. 4). Unifrac delineated between sampling sites, with only a few
161 exceptions. NI oysters clustered together, whereas OR oysters were dispersed among several
162 branches, indicating NI oyster microbiomes, which had overall fewer unique phlotypes than

163 OR, are overall more similar to each other than are OR oyster microbiomes. Unifrac analysis
164 revealed variance (see NI.7) that was not apparent in the dual-hierarchical clustering which
165 resulted from a classification level deeper than phylum. The OR water sample, which had the
166 lowest read coverage, was quite distant from most samples in both clustering analyses, with a
167 proportionally high number of reads assigned to the genus *Octadecabacter* (43.3%, compared to
168 the average of 0.2% for all other samples, ranging from 0.05% to 0.5%) and the Mamiellaceae
169 family (40.8%, compared to the average of 0.1% for all other samples, ranging from 0.002 to
170 0.5%).

171 The apparent differences in the oyster microbiome between the two sampling sites were
172 further interrogated by employing LEfSe to identify phlotypes that significantly differ by site.
173 The proportions of four phlotypes were significantly higher in OR oysters than NI oysters
174 including *Finegoldia*, *Bradyrhizobium*, *Roseateles depolymerans*, and *Brevundimonas*
175 *intermedia* (Fig. 5). In contrast, the proportions of eight phlotypes were significantly higher in
176 NI oysters compared to OR including *Propionigenium*, M2PT2_76, *Reinekea*, *Pseudomonas*
177 *viridiflava*, *Clostridium sticklandii*, *Vibrio fortis*, *Halobacillus yeomjeoni*, and
178 Endozoicimonaceae. *Finegoldia* is typical of the human gastrointestinal tract (28) and
179 *Bradyrhizobium* is a soil-dwelling, root nodule organism (29), so these associations with OR are
180 consistent with site being a narrow tidal tributary where the oyster bed is in close proximity to
181 the terrestrial environment and a WWTF outfall. Conclusions on associations by site of the other
182 organisms are not possible due to absence of relevant information in published studies.

183

184 2.3 Differences in predicted functional profiles between sites

185 In addition to defining the members of the oyster microbiome, we investigated potential
186 functional differences inferred from phylotype composition between the sampling sites, which
187 may be driven by their unique ecological and environmental associations. For this we used the
188 bioinformatics tool PICRUSt that draws upon previously sequenced genomes and annotations
189 (30). A total of 887 predicted gene functions significantly differed between NI and OR oyster
190 microbiomes ($p < 0.05$). Further examination of the functional differences of the 11 functions at
191 $p < 0.0005$ reveals two distinct classes (Fig. 6). OR oyster microbiomes had a higher number of
192 functions generally involved in cell growth, including nucleotide metabolism, tRNA synthesis
193 and associated elongation factors, amino acid biosynthesis, and oxidative phosphorylation. NI
194 oyster microbiomes had a higher number of diverse metabolic functions (sugar, chlorophyll,
195 carbon, and sulfur metabolism) as well as higher number of chaperone-associated proteins. The
196 more diverse photosynthesis related metabolic capacity logically related to the prevalence of 16s
197 sequences identified as Cyanobacteria at NI, as compared to OR. Overall, the variations between
198 microbiomes and their respective predicted functions at each site could relate to nutrient
199 conditions that support different types of organisms. The OR oyster bed not only is impacted by
200 a nearby municipal WWTF discharge, which could explain the slightly higher levels of dissolved
201 nutrients associated with WWTF effluent (orthophosphate, nitrate), but also more directly
202 influenced by rainfall/runoff events and nonpoint source pollution (Table 2). OR has higher
203 chlorophyll *a*, water temperature, and turbidity with lower salinity and dissolved oxygen
204 compared to NI (Table 2A&B). NI is also a much larger oyster bed with abundant oyster cultch
205 on coarser textured sediment compared to OR. The chronic loading of readily available nutrients
206 at OR may support more rapid total growth of a less diverse bacterial population, whereas the
207 lower, potentially limiting nutrient concentrations available at NI may support a more diverse

208 bacterial population, in agreement with the measures of alpha diversity (Fig. 1). This pattern of
209 overall lower taxonomic and function diversity in OR is in agreement with other studies that
210 indicate wastewater effluent decreases microbial diversity (31, 32).

211

212 2.4 Abundance of *V. parahaemolyticus* in individual oysters and correlations with 213 microbiome

214 To evaluate potential correlations of microbiome with *V. parahaemolyticus*, we applied a
215 quantitative qPCR-based MPN enumeration method of *V. parahaemolyticus* to individual oysters
216 (see methods), which allowed evaluation of correlations between relative abundance of *V.*
217 *parahaemolyticus* and phylotypes in individual oyster microbiomes. This approach revealed that
218 individual oysters, even from the same site, differed dramatically in abundance of *V.*
219 *parahaemolyticus* (Table 3) as reported by two other individual oyster studies (32, 34). Oysters
220 were subsequently categorized and grouped based on log₁₀ MPN/g abundance level, where the
221 means of each group significantly differed from the other groups (Low: 0.48, Medium: 1.16,
222 High: 2.51; $p < 0.0001$). *V. parahaemolyticus* was only captured via 16s sequencing in the
223 medium and high abundance level oysters from NI (Table 3), being an overall rare component of
224 the sequenced oyster microbiome. Whereas the estimated relative (16s) and absolute (MPN) *V.*
225 *parahaemolyticus* abundance did not match, there was agreement in the general pattern of
226 detection of *V. parahaemolyticus* 16s rRNA and abundance by enrichment-based MPN.

227 NI harbored the only oysters with high abundance level of *V. parahaemolyticus*, and also
228 harbored oysters with medium and low abundance level. In contrast, OR contained oysters with
229 only medium and low abundance level *V. parahaemolyticus*. Due to these differences in
230 distribution of *V. parahaemolyticus* abundance, we queried whether differences in ecology

231 between these sites could impact microbial communities including *Vibrios*. There are some
232 differences in long-term nutrient conditions (Table 2; 35) between the two sites. The
233 combination of higher chlorophyll *a*, turbidity, nutrients (Table 2) and temperature, with lower
234 salinity and dissolved oxygen levels (representing short-term environmental conditions averaged
235 over the 12 hours prior to oyster harvest) at OR are consistent with it being a tributary and other
236 distinctions between the two sites (Table 2A&B). Interestingly, although chlorophyll *a*
237 positively correlates with *V. parahaemolyticus* presence even in the GBE (3, 8), it was higher at
238 OR. It is not clearly apparent that any of these measured abiotic parameters drove higher levels
239 of *V. parahaemolyticus* at NI in a subset of oysters, or comparatively lower levels of *V.*
240 *parahaemolyticus* at OR, but it is further evidence supporting site differences as a likely
241 contributing factor in oyster microbial community variation.

242 To investigate whether microbial community members correlated with *V.*
243 *parahaemolyticus* abundance, microbiome data for individual oysters were analyzed with
244 Unifrac distance trees to determine similarity of the microbiome of oysters in the same MPN
245 abundance level group, separated by site. Branching patterns did not correspond with *V.*
246 *parahaemolyticus* abundance level, indicating there is no overall similarity in the microbial
247 community in *V. parahaemolyticus* high abundance level oysters. Despite a lack of clustering of
248 samples by *V. parahaemolyticus* abundance level, there were 24 phylotypes significantly higher
249 in number in high abundance level oysters, one phylotype in medium abundance level oysters,
250 and three in low abundance level oysters (Fig. 7). However, a caveat to this data and its
251 interpretation is that these were all rare phylotypes of which the proportion could be influenced
252 by depth of sequencing of the microbiome (Fig. 1), in addition to the relationships potentially
253 being confounded by site-specific differences. Specifically, the 19 phylotypes that were

254 exclusive to high abundance level oysters (and by default present in significantly higher
255 proportions) could be an artifact of oyster location in the estuary. As such, the influence of
256 estuary location on differences in the microbiome was most apparent from this study, and
257 correlations of microbiome with *V. parahaemolyticus* abundance await a more robust sample
258 size and greater microbiome sequencing depth.

259

260 3. Conclusions

261 Microbial community profiling of the microbiome and quantification of *Vibrio*
262 *parahaemolyticus* abundance of oysters and overlaying water from two naturally occurring
263 oyster beds revealed individual oysters and sites have different taxonomic and functional
264 microbiome profiles. These differences, likely influenced by distinctive ecology, is in general
265 agreement with other studies that conclude the microbiomes of marine animals are highly
266 specific based on individuals' surrounding habitat (23, 25) and diet (36). Even so, that the
267 microbiome composition and *Vibrio* abundance were so variable between individuals from the
268 same site allude to the potential that community-level interactions within an oyster impact the
269 risk of *Vibrio parahaemolyticus* achieving an infective population size. A better understanding of
270 these interactions could open new avenues for disease prevention.

271 Both culture-based and culture independent methods revealed *V. parahaemolyticus* did
272 not equally accumulate in individual oysters, despite the oyster's exposure to the same general
273 environmental conditions at each site. Therefore, the measured environmental conditions cannot
274 explain differences in *V. parahaemolyticus* levels between individual oysters. Bivalves actively
275 filter water based upon particle size (37), bacterial species (38), strains within the same species
276 with known or introduced (i.e., mutations) genetic variation (39-41), and even differentiate

277 between viral particles (42). The *V. parahaemolyticus* strains themselves may contain genetic
278 factors or phenotypic traits influencing uptake and/or depuration and it is possible different
279 strains are accumulated at different rates, much like *Vibrio vulnificus* (43). Through differential
280 killing of strains or variants, oyster hemocytes may also reduce the accumulation of certain *V.*
281 *parahaemolyticus* strains (44, 14).

282 The higher abundance of Cyanobacteria at NI may influence the abundance of other
283 phyla at this site (27). It may also explain the higher abundance of *V. parahaemolyticus* at NI.
284 Cyanobacteria and *V. cholerae* will associate (3), and *Vibrio* spp. make up as much as 6% of all
285 cultivable heterotrophic bacteria isolated from cyanobacterial blooms (27). In addition,
286 cyanobacterial-derived organic matter increases *Vibrio* abundance (3). This study indicates the
287 general approach of microbiome profiling may reveal phylotypes and functional differences
288 associated with *V. parahaemolyticus* abundance with deeper sampling.

289

290

291 4. Methods

292 4.1 Oyster Collection and Processing

293 One water and ten oyster samples were collected at low tide on September 1st, 2009 from
294 two distinct naturally-occurring oyster beds in the New Hampshire Great Bay Estuary (GBE).
295 Oysters were collected using oyster tongs whereas water samples were collected by submerging
296 capped sterile bottles ~0.5m below the water surface and uncapping to fill. Samples were
297 immediately stored on ice packs in coolers until laboratory processing. Individual oysters were
298 cleaned, aseptically shucked, and thoroughly homogenized with a surface disinfected (using 90%
299 ethanol and filter sterilized water) Tissue Tearor (Biospec Products, Bartlesville, OK). Most

300 Probable Number (MPN) analyses were performed on individual oyster homogenate and water
301 samples as described in Schuster *et al.* (45). In brief, samples were serially diluted tenfold into
302 Alkaline Peptone Water (APW) and incubated at 37°C for 16 hours, and the tubes scored by
303 turbidity. To positively identify the presence of *V. parahaemolyticus*, 1.0mL of each turbid
304 dilution was pelleted, and the DNA obtained by organic extraction (46). The DNA was subjected
305 to a quantitative q-PCR based MPN as described below, to determine whether each turbid
306 dilution was positive for *V. parahaemolyticus*. The microbiome was recovered from water
307 samples following centrifugation in a 5810R centrifuge (Eppendorf, Hamburg, Germany) at
308 4,000 rpm and the supernatant discarded. The water bacterioplankton pellet and un-enriched
309 oyster homogenate not immediately used for MPN analysis were frozen at -80°C.

310

311 4.2 MPN/g enumeration

312 MPN tubes were scored as positive for *V. parahaemolyticus* by detection of the
313 thermolabile hemolysin gene (*tlh*) with q-PCR (47). The reaction contained 1x iQ Supermix
314 SYBR Green I (Bio-Rad, Hercules, CA) and 2µL of the DNA template in a final volume of 25µL.
315 An iCycler with the MyiQ Single Color Real-Time PCR Detection system with included
316 software (Bio-Rad, Hercules, CA, USA) was used with the published cycling parameters (48). A
317 melting curve was performed to ensure positive detection of the correct amplicon compared to a
318 control DNA sample (*V. parahaemolyticus* F11-3A). MPN tubes were scored as positive or
319 negative based on whether q-PCR starting quality values were below (negative) or above
320 (positive) the threshold value determined by the standard curve using purified F11-3A and water
321 blank with iCycler software. The *V. parahaemolyticus* MPN/g was calculated for each oyster

322 according the FDA BAM (24) and grouped by high, medium, or low abundance level based on
323 10-fold differences in MPN/g.

324

325 4.3 16s rDNA marker preparation

326 DNA was isolated from archived oyster homogenates. The homogenates were thawed on
327 ice for 10 minutes, the top ~1cm was aseptically removed and discarded, and 1.0g of each oyster
328 homogenate was aseptically collected. The entire bacterioplankton pellet was used for the water
329 samples. The total bacterial DNA was extracted using the E.Z.N.A. Soil DNA Kit (Omega Bio-
330 Tek, Norcross, GA, USA) following standard protocols for Gram-negative and -positive bacterial
331 isolation.

332 The V2 to V3 region of 16s rRNA gene (250bp) was amplified from each individual
333 sample in triplicate using PCR with standard 16s F8 (5' – AGTTTGATCCTGGCTCAG – 3')
334 with GS FLX Titanium Primer A (5' – CGTATCGCCTCCCTCGCGCCATCAG – 3') and R357
335 (5' – CTGCTGCCTYCCGTA – 3') with Primer B (5' –
336 CTATGCGCCTTGCCAGCCCGCTCAG – 3'), with each pair of corresponding forward and
337 reverse primer sets having a unique 6bp MID tag (48). The PCR reaction containing 45µL
338 Platinum PCR Supermix (Invitrogen, Carlsbad, CA, USA), 3µL of sample DNA, and 2µL
339 molecular grade water, was ran in an iCycler thermocycler (Bio-Rad, Hercules, CA, USA) at the
340 following conditions: 94°C for 90 seconds; 30 cycles of 94°C for 30 seconds, 50.7°C for 45
341 seconds, 72°C for 30 seconds; and 72°C for 3 minutes. The triplicate samples were combined
342 and then purified using the MinElute PCR Purification Kit (Qiagen, Valencia, CA, USA)
343 following standard protocols. Each purified sample was visualized on a 1.2% agarose gel to
344 ensure purity and quality including expected amplicon size.

345 A 10ng/mL multiplexed sample was prepared for the Roche Genome Sequencer FLX
346 System using Titanium Chemistry (454 Life Sciences, Branford, CT, USA). The DNA
347 concentration for each sample was quantified using a NanoDrop 2000c (Thermo Scientific,
348 Wilmington, DE, USA) and pooled with equal proportions of the twenty oyster and two water
349 samples. The pooled mixture was purified using the AMPure XP Purification Kit (Beckman
350 Coulter Genomics, Danvers, MA, USA) by manufacturers protocols, with the final samples
351 suspended in 20uL elution buffer EB from the MinElute PCR Purification Kit (Qiagen, Valencia,
352 CA, USA). The pooled tagged single-stranded pyrosequencing library underwent fusion PCR
353 and pyrosequencing using a Roche 454 FLX Pyrosequencer (454 Life Sciences, Branford, CT,
354 USA) according to the manufacturer instructions at the University of Illinois W.M. Keck Center
355 High-Throughput DNA Sequencing Center.

356

357 4.4 Community analysis

358 The forward 454 pyrosequencing reads were quality filtered and denoised to reduce
359 erroneous PCR and sequencing errors using FlowClus, setting zero primer and barcode
360 mismatches, a minimum sequence length of 200, zero ambiguous bases and seven
361 homopolymers allowed before truncation, a minimum average quality score of 25, and k=5 for
362 the flow value multiple (49). These sequences were then further filtered and clustered with
363 mothur 1.22.0 (50). The mothur workflow followed the 454 SOP accessed September 2014 (50)
364 with some modifications. The pre-clustering step was performed permitting one difference.
365 Chloroplasts were retained, as cyanobacteria have previously been identified as part of the oyster
366 microbiome (18, 23). The Greengenes 13.8 (51) reference database was used to assign taxonomy
367 to OTUs. After removing singleton OTUs, mothur 1.33.0 (50) was used to generate a distance

368 matrix, pick representative OTUs, and create a phylogenetic tree using clear-cut 1.0.9 (52) for
369 determining alpha diversity.

370 Rarified alpha diversity measurements were calculated with QIIME 1.8 (53) to determine
371 both the within-sample diversity and sequencing depth using whole-tree phylogenetic diversity
372 (PD) calculated with ten iterations of 100 reads added at each rarefaction step, up to 75% of the
373 sample with the highest number of reads (Supplemental Table 1). The distribution of OTUs
374 between sampling sites and substrates was determined with Venny 1.0 (54). Patterns in
375 abundance in phyla-level classifications in all samples were revealed with a dual-hierarchical
376 clustering performed with JMP 12 (SAS Institute Inc., Cary, North Carolina, USA) for log-
377 transformed percent abundance using both standardized and unstandardized average linkage.
378 Weighted and normalized Fast Unifrac (55), which uses all levels of taxonomic assignment to
379 create a distance matrix and groups samples based on similarity, was used to perform beta
380 diversity clustering and jackknife analyses for samples, jackknifing at 1000 permutations at 75%
381 of the sample with the lowest number of reads. LEfSe (56), PICRUS_t (30) and STAMP (57)
382 were all used at default settings, to determine taxonomic and profile similarities between sample
383 groups, and calculate statistical significance, respectively, pre-normalizing samples to 1M in
384 LEfSe.

385 To compare the sequenced-based abundance of *V. parahaemolyticus* to abundance
386 quantified with the culture-based MPN method, all quality-filtered, de-noised reads were aligned
387 to the region of *V. parahaemolyticus* strain RIMD 2210633 (GCA_000196095.1) that would be
388 amplified by the F8-R357 primer pair at 99.0% with PyNast (58) through QIIME 1.8 (54). The
389 identity of matching sequences was confirmed with BLAST (59).

390 Environmental and nutrient conditions per each site were assessed from the NOAA National
391 Estuarine Research Reserve System (<http://nerrs.noaa.gov/>) that measures conditions every 15
392 minutes.

393 Environmental data used in the statistical analyses were collected as part of this study and the
394 Great Bay National Estuarine Research Reserve (GBNERR) System Wide Monitoring Program
395 (SWMP). Water temperature, salinity, dissolved oxygen, pH, and turbidity were measured and
396 downloaded from YSI datasondes deployed at the study sites from April-December with 15-
397 minute readings. In addition, grab samples collected monthly by GBNERR SWMP were
398 analyzed for chlorophyll *a*, orthophosphate, ammonium, nitrate-nitrite and total dissolved
399 nitrogen (<http://cdmo.baruch.sc.edu/get/export.cfm>) Short-term environmental conditions,
400 including temperature, salinity, dissolved oxygen, pH, and turbidity were averaged for the 12
401 hours prior to sampling. Long-term nutrient patterns were assessed by averaging all nutrient
402 analysis data from 2007-2013. The fieldwork performed in this study did not involve endangered
403 or protected species.

404

405 **5. Acknowledgements**

406 We thank C Ellis and A Tyzik for assistance with MPNs, J Jarett and J Gaspar for assistance
407 with bioinformatics software, and W. K. Thomas for discussions. Partial funding for this was
408 provided by the USDA National Institute of Food and Agriculture Hatch NH00574, NH00609
409 (accession 233555) and NH00625 (accession 1004199). Additional funding provided by the
410 National Oceanic and Atmospheric Administration College Sea Grant program and grants R/CE-
411 137, R/SSS-2, R/HCE-3. Support also provided through the National Institutes of Health

412 1R03AI081102-01, and National Science Foundation EPSCoR IIA-1330641. This is Scientific
413 Contribution Number 2717 for the New Hampshire Agricultural Experiment Station.

414

415 **REFERENCES**

416 (1) Newton AE, Kendall M, Vugia DJ, Henao OL, Mahon BE. Increasing rates of vibriosis in the
417 United States, 1996–2010: Review of surveillance data from 2 systems. *Clin Infect Dis.* 2012;
418 54(5): S391–S395.

419

420 (2) FDA. Appendix 5: FDA and EPA Safety Levels in Regulations and Guidance. Available:
421 <http://www.fda.gov/downloads/Food/GuidanceRegulation/UCM252448.pdf>. Accessed 18
422 December 2015.

423

424 (3) Takemura AF, Chien DM, Polz MF. Associations and dynamics of *Vibrio*aceae in the
425 environment, from the genus to the population level. *Front Microbiol.* 2014; 5: 38.

426

427 (4) Larsen AM, Rikard FS, Walton WC, Arias CR. Temperature effect on high salinity
428 depuration of *Vibrio vulnificus* and *V. parahaemolyticus* from the eastern oyster (*Crassostrea*
429 *virginica*). 2015. *Int J Food Microbiol* 192:66-71.

430

431 (5) Parveen S, Jahncke M, Elmahdi S, Crocker H, Bowers J, White C, Gray S, Morris AC,
432 Brohawn K. High salinity relaying to reduce *Vibrio parahaemolyticus* and *Vibrio vulnificus* in
433 Chesapeake Bay oysters (*Crassostrea virginica*). 2017. *J Food Sci.* 82:484-491.

434

- 435 (6) Yu JW. Incidence, abundance, post-harvest processing and population diversity of pathogeni
436 Vibrios in oysters from the Great Bay Estuary. University of New Hampshire, ProQuest
437 Dissertations Publishing, 2011. 1507840
438
- 439 (7) Main CR, Salvitti LR, Whereat EB, Coyne KJ. Community-level and species-specific
440 associations between phytoplankton and particle-associated *Vibrio* species in Delaware's inland
441 bays. *Appl Environ Microbiol.* 2015; 81(17): 5703-5713
442
- 443 (8) Urquhart EA, Jones SH, Yu JW, Schuster BM, Marcinkiewicz AL, Whistler CA, et al.
444 Environmental conditions associated with elevated risk conditions for *Vibrio parahaemolyticus*
445 in the Great Bay Estuary, NH. *PLoS ONE.* 2015; 11(5): e0155018.
446
- 447 (9) Matz C, Nouri B, McCarter L, Martinez-Urtaza J. Acquired type III secretion system
448 determines environmental fitness of epidemic *Vibrio parahaemolyticus* in the interaction with
449 bacteriivorous protists. 2011. *PloS One* 6:e20275
450
- 451 (10) Lokmer A, Goedknecht MA, Thielges DW, Fiorentino D, Kuenzel S, Baines JF, Wegner
452 KM. Spatial and temporal dynamics of Pacific oyster hemolymph microbiota across multiple
453 scales. 2016 7:13678
454
- 455 (11) Givens CE, Bowers JC, DePaola A, Hollibaugh JT, Jones JL. Occurrence and distribution of
456 *Vibrio vulnificus* and *Vibrio parahaemolyticus* – potential roles for fish, oyster, sediment, and
457 water. *Letters in Appl Microbiol.* 2014; 58(6): 503-510.

458

459 (12) Olafsen JA, Mikkelsen HV, Giaever HM, Hansen GH. Indigenous bacteria in hemolymph
460 and tissues of marine bivalves at low temperatures. *Appl Environ Microbiol*. 1993; 59(6): 1848-
461 1854.

462

463 (13) Pujalte MJ, Ortigosa M, Maciá MC, Garay E. Aerobic and facultative anaerobic
464 heterotrophic bacteria associated to Mediterranean oysters and seawater. *Int Microbiol*. 1999;
465 12(4): 259-266.

466

467 (14) Volety AK, McCarthy SA, Tall BD, Curtis SK, Fisher WS, Genthner FJ. Responses of
468 oyster *Crassostrea virginica* hemocytes to environmental and clinical isolates of *Vibrio*
469 *parahaemolyticus*. *Aquat Microb Ecol*. 2001; 25: 11-20.

470

471 (15) Long, RA, Azam F. Antagonistic interactions among marine pelagic bacteria. *Appl Environ*
472 *Microbiol*. 2001; 67(11): 4975-4983.

473

474 (16) Rypien KL, Ward JR, Azam F. Antagonistic interactions among coral-associated bacteria.
475 *Environ Microbiol*. 2009; 12(1): 28-39.

476

477 (17) Frydenborg, BR, Krediet CJ, Teplitski M, Ritchie KB. Temperature-dependent inhibition of
478 opportunistic *Vibrio* pathogens by native coral commensal bacteria. *Microb Ecol*. 2014; 67(2):
479 392-401.

480

481 (18) Chauhan A, Wafula D, Lewis DE, Pathak A. Metagenomic assessment of the eastern oyster-
482 associated microbiota. *Genome Announc.* 2014; 2(5): e01083-14.

483

484 (19) Chen H, Liu Z, Wang M, Chen S, Chen T. Characterization of the spoilage bacterial
485 microbiota in oyster gills during storage at different temperatures. *J Sci Food Agric.* 2013;
486 93(15): 3748-3754.

487

488 (20) King GM, Judd C, Kuske CR, Smith C. Analysis of stomach and gut microbiomes of the
489 eastern oyster (*Crassostrea virginica*) from coastal Louisiana, USA. *PLoS ONE.* 2012; 7(12):
490 e51475.

491

492 (21) Trabal-Fernandez N, Mazon-Suastegui JM, Vazquez-Juarez R, Ascencio-Valle F, Romero J.
493 Changes in the composition and diversity of the bacterial microbiota associated with oysters
494 (*Crassostrea corteziensis*, *Crassostrea gigas* and *Crassostrea sikamea*) during commercial
495 production. *FEMS Microbiol Ecol.* 2013; 88: 69-83.

496

497 (22) Wegner KM, Volkenborn N, Peter H, Eiler A. Disturbance induced decoupling between host
498 genetics and composition of the associated microbiome. *BMC Microbiol.* 2013; 13: 252.

499

500 (23) Zurel D, Benayahu Y, Or A, Kovacs A, Gophna U. Composition and dynamics of the gill
501 microbiota of an invasive Indo-Pacific oyster in the eastern Mediterranean Sea. *Environ*
502 *Microbiol.* 2011; 13(6): 1467-1476.

503

- 504 (24) FDA. Bacteriological analytical manual. Chapter 9. *Vibrio*. Kaysner, CA and A. DePaola.
505 <http://www.fda.gov/Food/FoodScienceResearch/LaboratoryMethods/ucm2006949.htm>.
506 Accessed 8 March 2016.
507
- 508 (25) Thomas IV JC, Wafula D, Chauhan A, Green SJ, Gragg R, Jagoe C. A survey of deepwater
509 horizon (DWH) oil-degrading bacteria from the Eastern oyster biome and its surrounding
510 environment. *Front Microbiol.* 2009; 5: 149.
511
- 512 (26) Avila-Poveda OH, Torres-Ariño A, Girón-Cruz DA, Cuevas-Aquirre A. Evidence for
513 accumulation of *Synechococcus elongatus* (Cyanobacteria: Cyanophyceae) in the tissues of the
514 oyster *Crassostrea gigas* (Mollusca: Bivalvia). *Tissue Cell.* 2014; 46(5): 379-387.
515
- 516 (27) Berg KA, Lyra C, Sivonen K, Paulin L, Suomalainen S, Tuomi P, et al. High diversity of
517 cultivable heterotrophic bacteria in association with cyanobacterial water blooms. *ISME J.* 2009;
518 3(3): 314-325.
519
- 520 (28) Levy P-Y, Fenollar F, Stein A, Borrión F, Raoult D. *Finegoldia magna*: a forgotten
521 pathogen in prosthetic joint infection rediscovered by molecular biology. *Clin Infect Dis.* 2009;
522 49(8): 1244-1247.
523
- 524 (29) Jordan DC. NOTES: Transfer of *Rhizobioum japonicum* Buchanan 1980 to *Brazyrhizobium*
525 gen. nov., a genus of slow-growing, root nodule bacteria from leguminous plants. *Int J Syst Evol*
526 *Microbiol.* 1982; 32: 136-139.

527

528 (30) Langille MGI, Zaneveld J, Caporaso JG, McDonald D, Knights D, Reyes JA, et al.

529 Predictive functional profiling of microbial communities using 16S rRNA marker gene

530 sequences. *Nat Biotechnol.* 2013; 31: 814-821.

531

532 (31) Drury B, Rosi-Marshall E, Kelly JJ. Wastewater treatment effluent reduces the abundance

533 and diversity of benthic bacterial communities in urban and suburban rivers. *Appl Environ*

534 *Microbiol.* 2013; 79(6): 1897-1905.

535

536 (32) Li D, Sharp JO, Drewes JE. Influence of wastewater discharge on the metabolic potential of

537 the microbial community in river sediments. *Microb Ecol.* 2016; 71(1): 78-86.

538

539 (33) Kaufman GE, Bej AK, DePaola A. Oyster-to-oyster variability in levels of *Vibrio*

540 *parahaemolyticus*. *J Food Prot.* 2003; 66(1): 125-129.

541

542 (34) Klein SL, Lovell CR. The Hot oyster: levels of virulent *Vibrio parahaemolyticus* strains in

543 individual oysters. 2017 93(2) pii:fiw232

544

545 (35) Jones SH, Summer-Brason BW. 1998. Incidence and detection of pathogenic *Vibrio* sp. in a

546 northern New England estuary, USA. *J. Shellfish Res.* 17:1665–1669.

547

548 (36) Givens CE, Ransom B, Bano N, Hollibaugh JT. Comparison of the gut microbiomes of 12

549 bony fish and 3 shark species. *Mar Ecol Prog Ser.* 2015; 518: 209-223.

550

551 (37) Ward JE, Shumway SE. Separating the grain from the chaff: particle selection in
552 suspension- and deposit-feeding bivalves. *J Exp Mar Biol Ecol.* 2004; 300: 83-130.

553

554 (38) Birkbeck TH, McHenry JG. Degradation of bacteria by *Mytilus edulis*. *Marine Biol.* 1982;
555 72: 7-15.

556

557 (39) Murphree RL, Tamplin ML. Uptake and retention of *Vibrio cholerae* O1 in the Eastern
558 oyster, *Crassostrea virginica*. *Appl Environ Microbiol.* 1995; 61(10): 3656-3660.

559

560 (40) Paranjpye RN, Johnson AB, Baxter AE, Strom MS. Role of type IV pilins in persistence of
561 *Vibrio vulnificus* in *Crassostrea virginica* oysters. *Appl Environ Microbiol.* 2007; 73(15): 5041-
562 5044.

563

564 (41) Srivastava M, Tucker MS, Gulig PA, Wright AC. Phase variation, capsular polysaccharide,
565 pilus, and flagella contribute to uptake of *Vibrio vulnificus* by the Eastern oyster (*Crassostrea*
566 *virginica*). *Environ Microbiol.* 2009; 11(8): 1934-1944.

567

568 (42) Soizick LG, Robert A, Haifa M, Jacques LP. Shellfish contamination by norovirus: strain
569 selection based on ligand expression?. *Clin Virol.* 2013; 41(1): 3-18.

570

571 (43) Froelich BA, Ringwood A, Sokolova I, Oliver JD. Uptake and depuration of the C- and E-
572 gneotypes of *Vibrio vulnificus* by the Eastern oyster (*Crassostrea virginica*). Environ Microbiol
573 Rep. 2009; 2(1): 112-115.

574

575 (44) Genther FJ, Volety AK, Oliver LM, Fisher WS. Factors influencing *in vitro* killing of
576 bacteria by hemocytes of the Eastern oyster (*Crassostrea virginica*). Appl Environ Microbiol.
577 1999; 65(7): 3015-3020.

578

579 (45) Schuster BM, Tyzik AL, Donner RA, Striplin MJ, Almagro-Moreno S, Jones SH, et al.
580 Ecology and genetic structure of a northern temperate *Vibrio cholerae* population related to
581 toxigenic isolates. Appl Environ Microbiol. 2011; 77(21): 7568-7575.

582

583 (46) Ausubel F, Brent R, Kingston RE, Moore DD, Seidman JG, Smith JA, et al. Current
584 protocols in molecular biology. New York, N.Y.: Wiley and Sons, Inc.; 1990.

585

586 (47) Nordstrom JL, Vickery MCL, Blackstone GM, Murray SL, DePaola A. Development of a
587 multiplex real-time PCR assay with an internal amplification control for the detection of total
588 and pathogenic *Vibrio parahaemolyticus* bacteria in oysters. Appl Environ Microbiol. 2007;
589 73(18): 5840-5847.

590

591 (48) Liu Z, Lozupone C, Hamady M, Bushman FD, Knight R. Short pyrosequencing reads
592 suffice for accurate microbial community analysis. Nucleic Acids Res. 2007; 35(18): e120-.

593

594 (49) Gaspar JM, Thomas WK. FlowClus: Efficiently filtering and denoising pyrosequenced
595 amplicons. *BMC Bioinformatics* 2015; 16: 105.

596

597 (50) Schloss PD, Westcott SL, Ryabin T, Hall JR, Hartmann M, Hollister EB, et al. Introducing
598 mothur: open-source, platform-independent, community-supported software for describing and
599 comparing microbial communities. *Appl Environ Microbiol.* 2009; 75(23): 7537-7541.

600

601 (51) DeSantis TZ, Hugenholtz P, Larsen N, Rojas M, Brodie EL, Keller K, et al. Greengenes, a
602 chimera-checked 16S rRNA gene database and workbench compatible with ARB. *Appl Environ*
603 *Microbiol.* 2006; 72(7): 5069-5072.

604

605 (52) Sheneman L, Evans J, Foster JA. Clearcut: A fast implementation of relaxed neighbor
606 joining. *Bioinformatics.* 2006; 22(22): 2823-2824.

607

608 (53) Caporaso JG, Kuczynski J, Stombaugh J, Bittinger K, Bushman FD, Costello EK, et al.
609 QIIME allows analysis of high-throughput community sequencing data. *Nat Meth.* 2010; 7(5):
610 335-336.

611

612 (54) Oliveros JC. Venny, an interactive tool for comparing lists with Venn's diagrams. 2007-
613 2015. <http://bioinfo.gp.cnb.csic.es/tools/venny/index.html>.

614

615 (55) Lozupone C, Lladser ME, Knights D, Stombaugh J, Knight R. UniFrac: an effective
616 distance metric for microbial community comparison. *ISME J.* 2011; 5(2): 169-172.

617

618 (56) Segata, N, Izard J, Waldron L, Gevers D, Miropolsky L, Garrett WS, et al. Metagenomic
619 biomarker discovery and explanation. *Genome Biol.* 2011; 12(6): R60.

620

621 (57) Parks DH, Tyson GW, Hugenholtz P, Beiko RG. STAMP: statistical analysis of taxonomic
622 and functional profiles. *Bioinformatics.* 2014; 30(1): 3123-3124.

623

624 (58) Caporaso JG, Bittinger K, Bushman FD, DeSantis TZ, Andersen GL, Knight R. PyNAST: A
625 flexible tool for aligning sequences to a template alignment. *Bioinformatics.* 2010; 26(2): 266-
626 267.

627

628 (59) Altschul SF, Gish W, Miller W, Myers EW, Lipman DJ. Basic local alignment search tool. *J*
629 *Mol Biol.* 1990; 215:403-410.

630

631

632

633 Figure Captions:

634

635 Figure 1. Rarified alpha diversity assessment. Phylogenetic Distance (PD) whole tree index for
636 individual oyster and overlying water samples were generated where each sample is represented
637 by a unique color.

638

639 Figure 2. Relationships between OTUs identified in oysters and overlying water from two
640 estuarine locations. (A) Distribution of all OTUs in water and in any oyster sample and (B)
641 distribution of all OTUs in water and in every oyster sample by site (OR or NI), representing the
642 site-specific and overall core microbiome.

643

644 Figure 3. Dual hierarchical analysis of phyla-level classification. The log-transformed percent
645 abundance of each phylum is indicated by a color scale. Samples and phyla are clustered based
646 on (A) unstandardized and (B) standardized average linkage. In unstandardized linkage, the
647 abundance of each phylum in a given sample is colored based on relative abundance of all phyla,
648 whereas in standardized the abundance of each phylum is colored based on the relative
649 abundance of that phylum across all samples.

650

651 Figure 4. Unifrac phylogenetic distance analysis. Phylogenetic distance of all taxonomic levels
652 for each pair of samples was calculated by the total branch length of unique phylotypes and
653 divided by total branch length of all phylotypes.

654

655 Figure 5. Effect size of phylotypes in oysters at significantly different proportions at each
656 collection site determined by LEfSe. LEfSe employs the non-parametric factorial Kruskal-Wallis
657 sum-rank, Wilcoxon rank-sum, and Linear Discriminant Analysis tests to determine the effect
658 size of significantly different phylotypes (56).

659

660 Figure 6. Distribution of Annotated functions at each site. (A) PICRUSt-derived KEGG
661 orthology IDs at significant different ($p < 0.0005$) numbers at each site, and (B) the pathways
662 associated with each ID.

663
664 Figure 7. PICRUSt-derived phylotypes in oysters at different proportions by *V.*
665 *parahaemolyticus* abundance class. Phylotypes followed by an * were only present in high
666 abundance oysters.

667
668 Table 1. OTU assignment to level of taxonomic classification following processing.
669

	OTUs classified at each taxonomic level (% of total)	
	QIIME	mothur
Unclassified	1524 (26.4)	0 (0)
Kingdom	4240 (73.6)	5756 (100)
Phylum	4227 (73.3)	5446 (94.6)
Class	4173 (72.4)	5411 (94.0)
Order	3676 (63.8)	4987 (86.6)
Family	2666 (46.3)	4363 (75.8)
Genus	863 (15.0)	3155 (54.8)
Species	74 (1.3)	2059 (35.8)

670
671
672
673
674
675
676
677
678
679
680
681
682
683
684
685

686 Table 2. Environmental conditions associated with collection sites

A. Average datasonde¹ measures during 12 hours prior to sampling on 8/31 to 9/1/09.

	Water	Salinity	Dissolved O ₂	O ₂	Turbidity	pH
	Temperature		Saturation	Concentration		
SITE	°C	ppt	%	mg/L	NTU/L	
OR	20.7	20.4	88.5	7.0	29.7	7.5
NI	19.9	23.2	95.3	7.6	6.4	7.5

B. Average concentrations in grab samples collected during July-August during 2007-2009.

	Orthophosphate	Ammonium	Nitrate/nitrite	Total dissolved N	Chlorophyll <i>a</i>
SITE	mg/L	mg/L	mg/L	mg/L	µg/L
OR	0.041	0.075	0.103	0.171	9.4
NI	0.031	0.067	0.032	0.096	5.7

687
688 ¹Data derived from a YSI datasonde deployed at each site with readings taken at 15 min
689 intervals. Ppt: parts per thousand; NTU: Nephelometric Turbidity Unit.

690

691

692

693

694

695

696

697

698 Table 3. Distribution of *Vibrio parahaemolyticus* in oysters as determined by MPN and 16s
699 sequencing¹.

Oyster	Log10 MPN/g	Abundance Level	16s Reads
NI.10	0.52	Low	-
NI.5	0.72	Low	-
NI.7	1.01	Medium	-
NI.8	1.01	Medium	2 (0.011)
NI.1	1.34	Medium	3 (0.020)
NI.6	1.34	Medium	-
NI.2	2.38	High	-
NI.3	2.38	High	2 (0.011)
NI.4	2.38	High	1 (0.003)
NI.9	2.88	High	1 (0.009)
OR.10	0.13	Low	-
OR.4	0.28	Low	-
OR.6	0.28	Low	-
OR.2	0.49	Low	-
OR.8	0.52	Low	-
OR.5	0.93	Low	-
OR.1	1.01	Medium	-
OR.3	1.01	Medium	-
OR.7	1.20	Medium	-
OR.9	1.34	Medium	-

700
701 ¹Oysters from Nannie Island (NI.1-10), and Oyster River (OR.1-10) are ordered by site and
702 within site by increasing *V. parahaemolyticus* abundance level as determined by MPN. 16s reads
703 represents the number of *V. parahaemolyticus* sequences and relative percent abundance in
704 parentheses

705
706

707

708

709

710

711

712

713 Supplemental Table 1. Reads available for analysis following quality filtering.

714

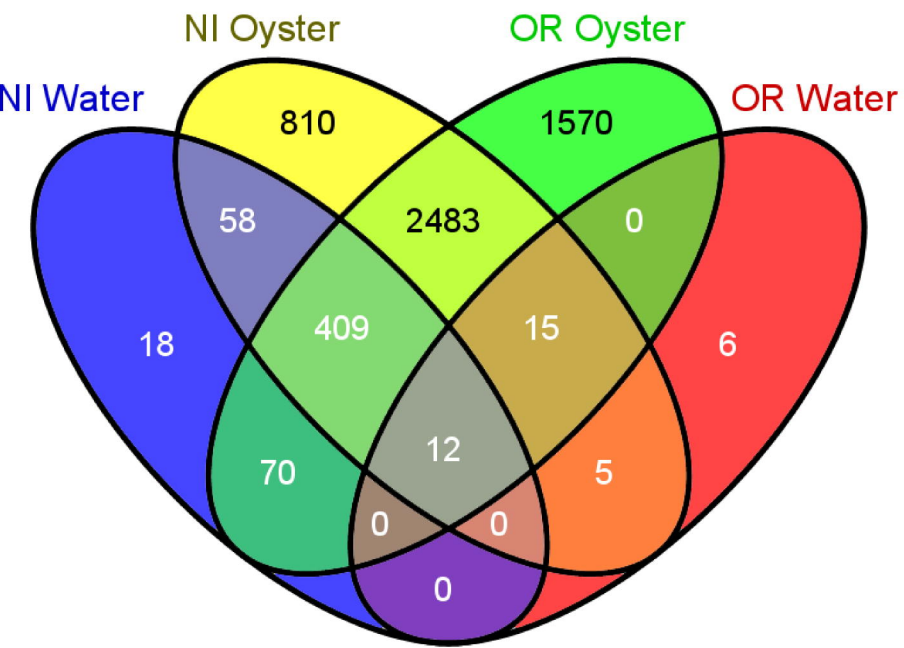
Oyster	NI	OR
1	14786	34420
2	17900	25737
3	17478	36390
4	31802	25115
5	12500	47231
6	10390	33229
7	21227	24765
8	17670	34639
9	21719	9672
10	15468	22802
Water	6495	397

715

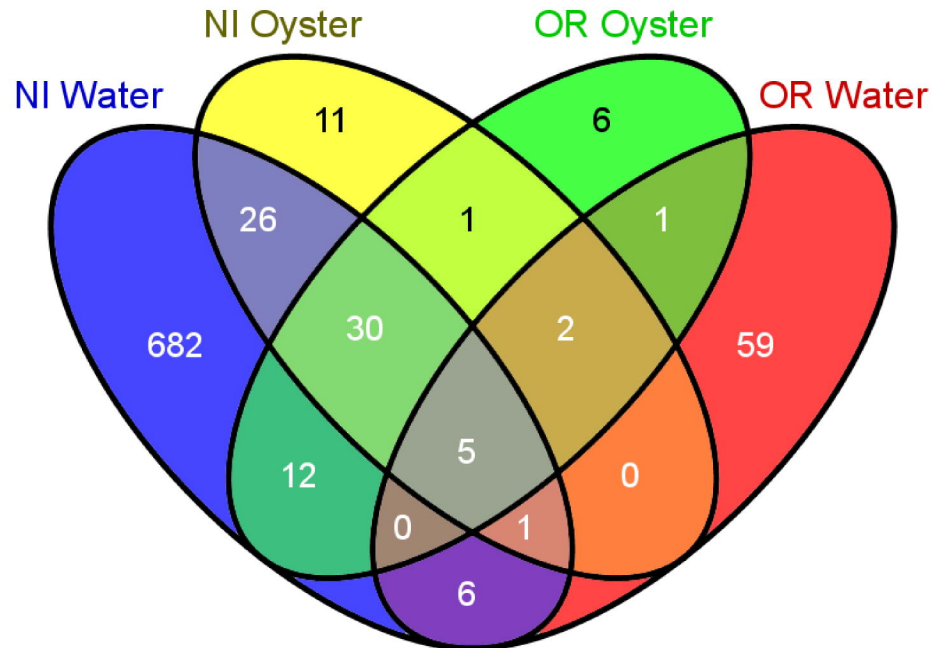
716

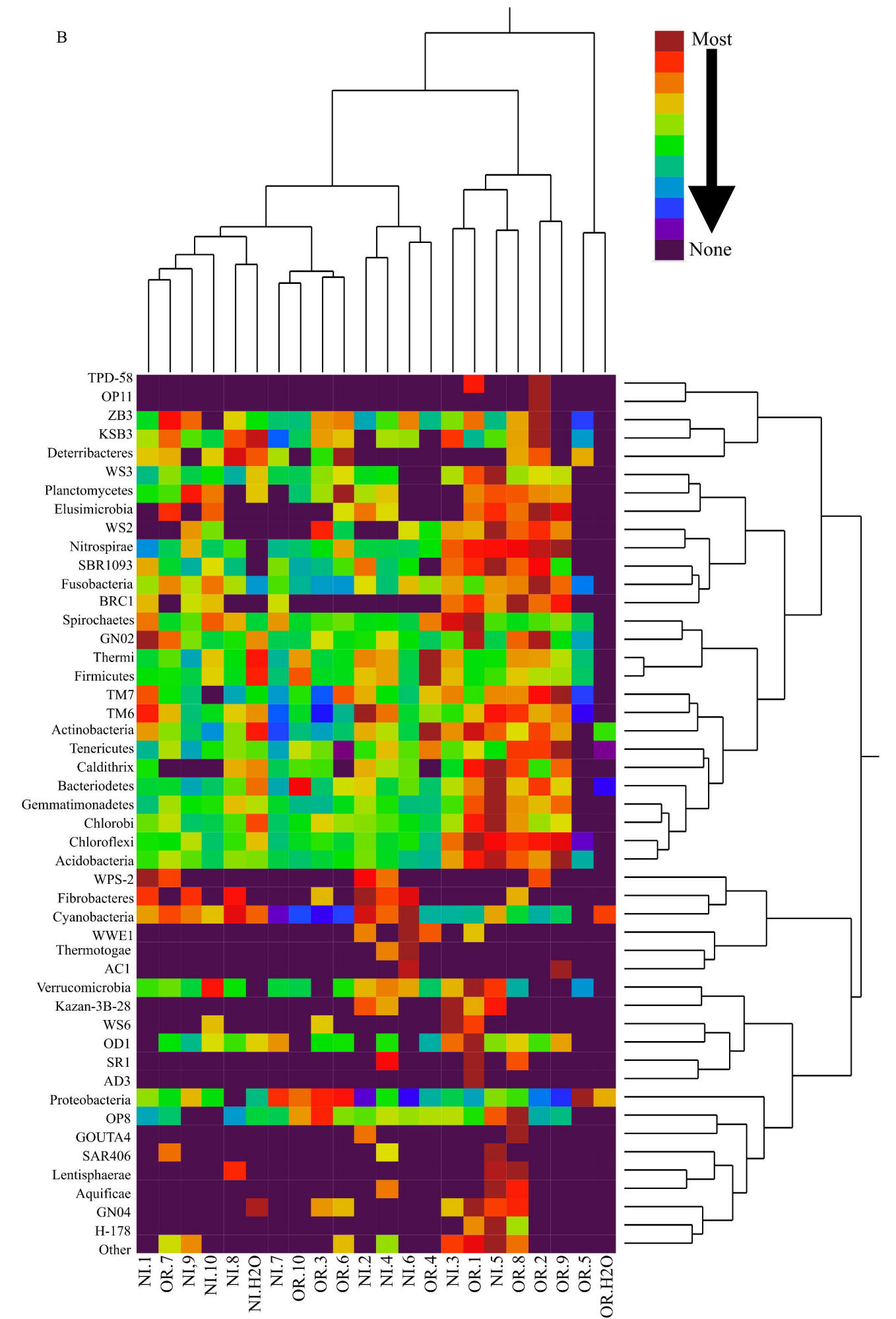
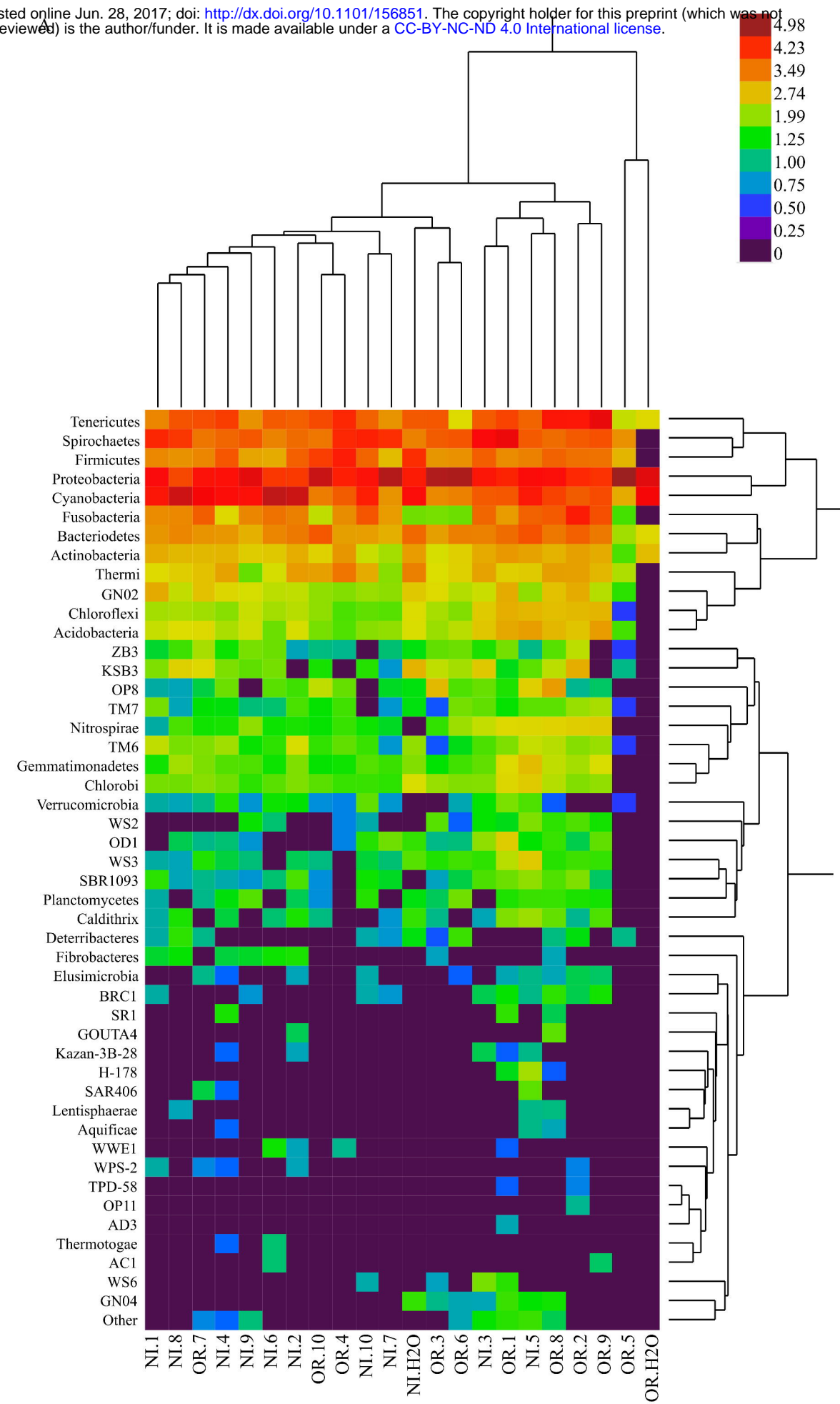
717

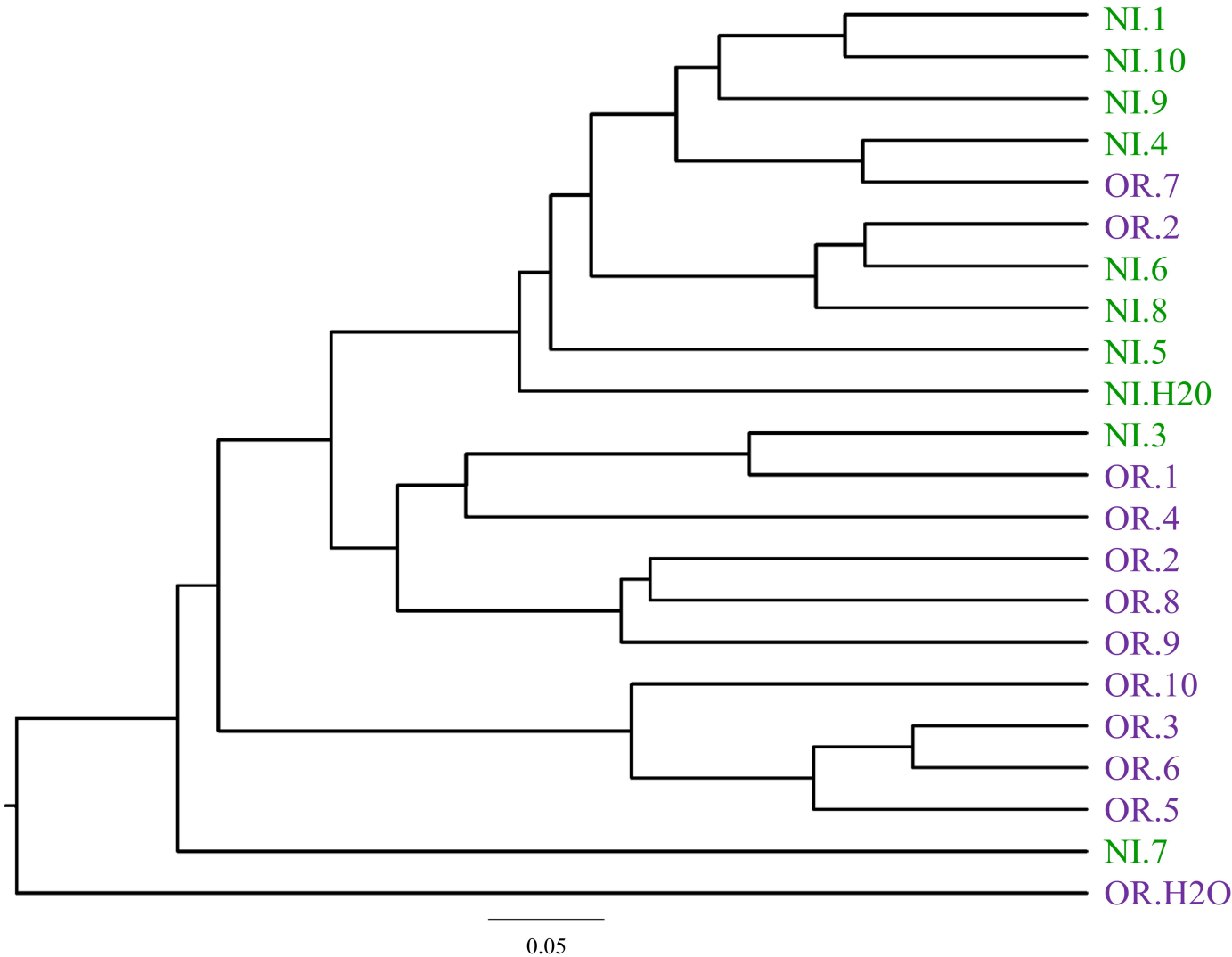
A



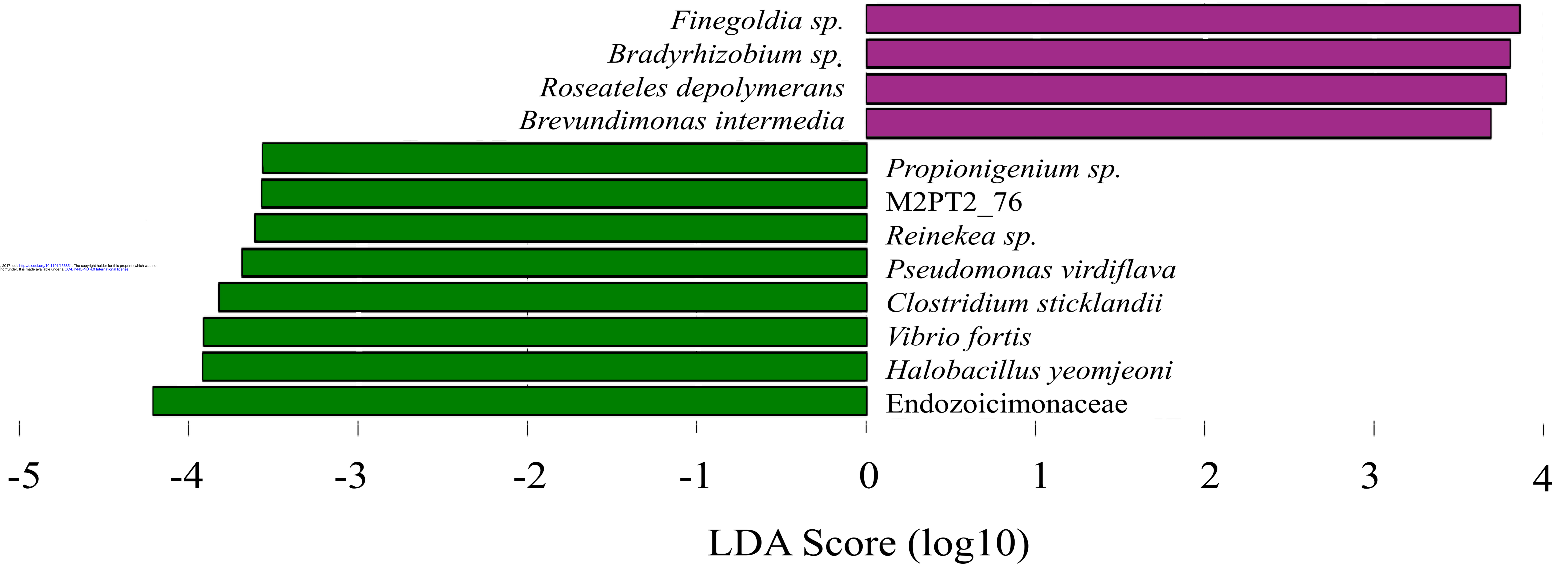
B



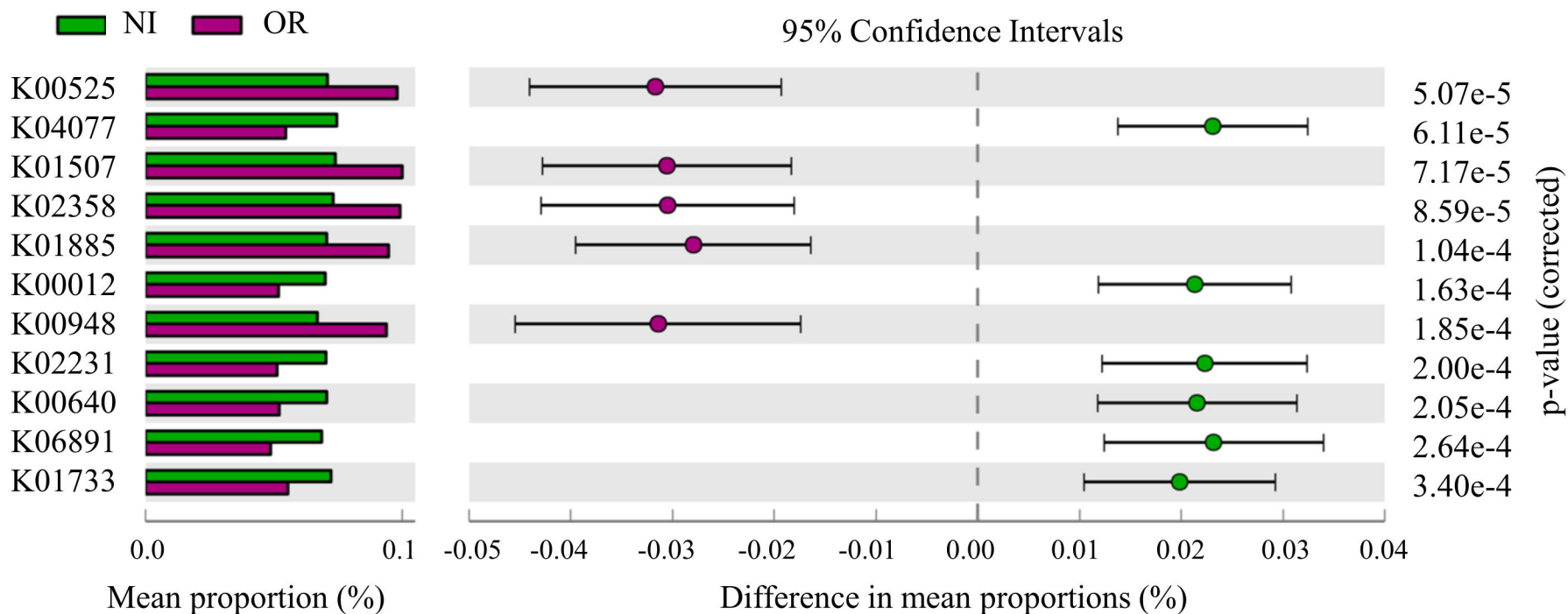




■ NI ■ OR



A



B

KEGG ID	Function
K00525	ribonucleoside-diphosphate reductase alpha chain [EC:1.17.4.1]
K04077	chaperonin GroEL
K01507	inorganic pyrophosphatase [EC:3.6.1.1]
K02358	elongation factor EF-Tu [EC:3.6.5.3];elongation factor Tu
K01885	glutamyl-tRNA synthetase [EC:6.1.1.17]
K00012	UDPglucose 6-dehydrogenase [EC:1.1.1.22]
K00948	ribose-phosphate pyrophosphokinase [EC:2.7.6.1]
K02231	adenosylcobinamide kinase / adenosylcobinamide-phosphate guanylyltransferase [EC:2.7.1.156 2.7.7.62]
K00640	serine O-acetyltransferase [EC:2.3.1.30]
K06891	ATP-dependent Clp protease adaptor protein ClpS
K01733	threonine synthase [EC:4.2.3.1]

High Low Medium

